SAGA–HE–99
February 10, 1996

Numerical Approach to CP-Violating Dirac Equation

arXiv:hep-ph/9602269v1 10 Feb 1996

Koichi Funakubo[a,1], **Akira Kakuto**[b,2],
Shoichiro Otsuki[b,3] **and Fumihiko Toyoda**[b,4]

[a)] *Department of Physics, Saga University, Saga 840 Japan*

[b)] *Department of Liberal Arts, Kinki University in Kyushu, Iizuka 820 Japan*

Abstract

We propose a new method to evaluate the chiral charge flux, which is converted into baryon number in the framework of the charge transport scenario of electroweak baryogenesis. By the new method, one can calculate the flux in the background of any type of bubble wall with any desired accuracy.

[1]e-mail: funakubo@cc.saga-u.ac.jp
[2]e-mail: kakuto@fuk.kindai.ac.jp
[3]e-mail: otks1scp@mbox.nc.kyushu-u.ac.jp
[4]e-mail: ftoyoda@fuk.kindai.ac.jp

1 Introduction

In the scenario of electroweak baryogenesis[1], the chiral charge flux, which is converted to baryon number by the sphaleron process, is one of key ingredients. That is supposed to be generated by two mechanisms, both of which depend on the interaction of the fermions with the CP-violating background of the bubble wall created at the electroweak phase transition (EWPT). One of the mechanisms is the charge transport scenario, which is quantum mechanical and effective for thin walls, the other is the spontaneous baryogenesis, which is classical and effective for thick walls.

As for the charge transport scenario, the flux is determined by the difference in the reflection coefficients of the left- and right-handed fermions, as well as by that in the distribution functions in the broken and the symmetric phases divided by the bubble wall. The reflection coefficients are calculated by solving the Dirac equation in the background of the bubble wall, which is accompanied spatially varying CP violation. Cohen, *et al.*[2] first evaluated the flux by solving the Dirac equation numerically, assuming the kink-type profile for the modulus of the Higgs field and a function linear in the kink for the phase. On the other hand, we formulated a perturbative method applicable for small CP-violating phase and proved various relations among the reflection and transmission coefficients[3, 4]. Although it enables us to derive analytical relations, it can actually be applied only to the case in which the unperturbed Dirac equation is exactly solved and the CP-violating phase is sufficiently small. However the profile of the bubble wall should be determined by the dynamics of the EWPT. We pointed out, by solving the equations of motion for the gauge-Higgs system, that the CP-violating phase can be of $O(1)$ even if that is small in the broken phase at $T = 0$, according to the parameters in the effective potential[5]. For a larger CP-violating phase, we naively expect larger baryon number to be generated. So we need a method to evaluate the chiral charge flux for arbitrary profile of the bubble wall.

In [2], the one-dimensional Dirac equation is solved within a finite range $[0, z_0]$ including the bubble wall, imposing the boundary condition in which plane waves are injected at the boundary. Strictly, a plane wave is not an eigenfunction at any finite z, so that the choice of the range will affect the precision of the results. In this paper, we propose another procedure to solve the Dirac equation and to calculate the reflection and transmission coefficients. Although the method is numerical, its precision can be so controlled that one can obtain the results with any accuracy. In section 2, we write down the CP-violating Dirac equation and give the expressions of the reflection and transmission coefficients of the chiral fermions. The procedure of the numerical analysis is given in section 3, and it is applied to some profiles, including those which we found in [5] and

that in [2] for comparison, in section 4. The final section is devoted to summary and discussions.

2 CP-Violating Dirac Equation

2.1 The Dirac equation

We consider a fermion in the background of a complex scalar, to which it couples by a Yukawa coupling. For the scalar to have a nontrivial complex vacuum expectation value (VEV), we assume it is a part of an extended Higgs sector of the electroweak theory, such as MSSM or more general two-Higgs-doublet model. At the electroweak phase transition, the Higgs changes its VEV from zero to nonzero value near the bubble wall created if the phase transition is first order.

Then the Dirac equation describing such a fermion is

$$i\partial\!\!\!/\psi(x) - m(x)P_R\psi(x) - m^*(x)P_L\psi(x) = 0, \tag{2.1}$$

where $P_R = \frac{1+\gamma_5}{2}$,$P_L = \frac{1-\gamma_5}{2}$ and $m(x) = -f\langle\phi(x)\rangle$ is a complex-valued function of spacetime. Here f is the Yukawa coupling. When the radius of the bubble is macroscopic and the bubble is static or moving with a constant velocity, we can regard $m(x)$ as a static function of only one spatial coordinate:

$$m(x) = m(t, \mathbf{x}) = m(z).$$

Putting

$$\psi(x) = \mathrm{e}^{i\sigma(-Et+\mathbf{p}_T\cdot\mathbf{x}_T)}, \qquad (\sigma = +1 \text{ or } -1) \tag{2.2}$$

(2.1) is reduced to

$$\left[\sigma(\gamma^0 E - \gamma_T p_T) + i\gamma^3\partial_z - m_R(z) - i\gamma_5 m_I(z)\right]\psi_E(\mathbf{p}_T, z) = 0, \tag{2.3}$$

where

$$\begin{aligned} \mathbf{p}_T &= (p^1, p^2), \qquad \mathbf{x}_T = (x^1, x^2), \qquad p_T = |\mathbf{p}_T|, \qquad \gamma_T p_T = \gamma^1 p^1 + \gamma^2 p^2, \\ m(z) &= m_R(z) + i m_I(z). \end{aligned}$$

If we denote $E = E^* \cosh\eta$ and $p_T = E^* \sinh\eta$ with $E^* = \sqrt{E^2 - p_T^2}$, $\mathbf{p}_T$ in (2.3) can be eliminated by the Lorentz transformation $\psi \mapsto \psi' = \mathrm{e}^{-\eta\gamma^0\gamma_5}\psi$:

$$\partial_z\psi_E(z) = i\gamma^3\left[-\sigma E^*\gamma^0 + m_R(z) + i\gamma_5 m_I(z)\right]\psi_E(z). \tag{2.4}$$

In our work on the perturbative treatment of CP violation, we used the eigenspinor of γ^3, since unperturbative part of the Dirac equation contains only γ^3. Here we shall use the chiral representation of the γ-matrices as in [2]. So the expression of the Dirac equation is the same as that in [2], but we write it for self-containedness.

In the chiral basis, the γ-matrices are represented as

$$\gamma^0 = \begin{pmatrix} 0 & -1 \\ -1 & 0 \end{pmatrix}, \quad \gamma^k = \begin{pmatrix} 0 & \sigma_k \\ -\sigma_k & 0 \end{pmatrix}, \quad \gamma_5 = \begin{pmatrix} 1 & 0 \\ 0 & -1 \end{pmatrix}.$$

If we write the four-spinor as

$$\psi_E(z) = \begin{pmatrix} \psi_1(z) \\ \psi_2(z) \\ \psi_3(z) \\ \psi_4(z) \end{pmatrix},$$

the Dirac equation is decomposed into two two-component equations:

$$\partial_z \begin{pmatrix} \psi_1(z) \\ \psi_3(z) \end{pmatrix} = i \begin{pmatrix} \sigma E^* & m^*(z) \\ -m(z) & -\sigma E^* \end{pmatrix} \begin{pmatrix} \psi_1(z) \\ \psi_3(z) \end{pmatrix}, \tag{2.5}$$

$$\partial_z \begin{pmatrix} \psi_4(z) \\ \psi_2(z) \end{pmatrix} = i \begin{pmatrix} \sigma E^* & m(z) \\ -m^*(z) & -\sigma E^* \end{pmatrix} \begin{pmatrix} \psi_4(z) \\ \psi_2(z) \end{pmatrix}. \tag{2.6}$$

Now let us introduce dimensionless parameters. Suppose that a is the parameter of mass dimension, whose inverse characterizes the width of the bubble wall. We shall comment on practical choice of it in the later section. Then put

$$\begin{aligned} x &\equiv az, \\ \epsilon &\equiv E^*/a, \\ \xi(x)\mathrm{e}^{i\theta(x)} &\equiv m(z)/a \end{aligned} \tag{2.7}$$

Since we are interested in the bubble wall background, the $m(z)$ is supposed to behave as

$$\begin{aligned} m(z) &\to m_0\mathrm{e}^{i\theta_0}, \qquad \text{as } z \to +\infty, \\ m(z) &\to 0, \qquad \text{as } z \to -\infty, \end{aligned}$$

where m_0 is the fermion mass and θ_0 is the CP-violating angle in the broken phase at the phase transition. We also put

$$\xi \equiv m_0/a. \tag{2.8}$$

In terms of these dimensionless parameters, the Dirac equation is expressed as

$$\partial_x \begin{pmatrix} \psi_1(x) \\ \psi_3(x) \end{pmatrix} = i \begin{pmatrix} \sigma\epsilon & \xi(x)\mathrm{e}^{-i\theta(x)} \\ -\xi(x)\mathrm{e}^{i\theta(x)} & -\sigma\epsilon \end{pmatrix} \begin{pmatrix} \psi_1(x) \\ \psi_3(x) \end{pmatrix}, \tag{2.9}$$

$$\partial_x \begin{pmatrix} \psi_4(x) \\ \psi_2(x) \end{pmatrix} = i \begin{pmatrix} \sigma\epsilon & \xi(x)\mathrm{e}^{i\theta(x)} \\ -\xi(x)\mathrm{e}^{-i\theta(x)} & -\sigma\epsilon \end{pmatrix} \begin{pmatrix} \psi_4(x) \\ \psi_2(x) \end{pmatrix}. \tag{2.10}$$

This is the equation we shall numerically analyze.

Before investigating the Dirac equation, let us write down the chiral currents in our basis. They are defined by

$$\begin{aligned} j_L^\mu(x) &= \bar{\psi}(x)\gamma^\mu \frac{1-\gamma_5}{2}\psi(x), \\ j_R^\mu(x) &= \bar{\psi}(x)\gamma^\mu \frac{1+\gamma_5}{2}\psi(x). \end{aligned}$$

It is easy to see that the relevant currents are written as

$$j_L^3(x) = |\psi_4(x)|^2 - |\psi_3(x)|^2, \tag{2.11}$$

$$j_R^3(x) = |\psi_1(x)|^2 - |\psi_2(x)|^2. \tag{2.12}$$

The asymptotic forms of these currents will be used to calculate the transmission and reflection coefficients.

2.2 Extraction of the oscillating factor

Here, for definiteness, we consider a scattering state in which the incident wave is coming from the symmetric phase region ($x \sim -\infty$) so that there is only the transmitted wave (right moving) in the broken phase ($x \sim +\infty$). This boundary condition is expressed as

$$\psi_a(x) \propto \mathrm{e}^{\sigma\alpha x} \qquad \text{as } x \to +\infty,$$

where $\alpha = i\sqrt{\epsilon^2 - \xi^2}$ and a denote the spinor index. Our aim is to find out the coefficients of the right and left movers in the symmetric phase region of this state, from which we can evaluate the chiral transmission and reflection coefficients.

For this purpose, we numerically integrate the Dirac equation starting from the plane wave in the deep broken phase, $x = +\infty$. However it is rather difficult to implement this situation numerically, since preparing the plane wave at $x = \infty$ is impossible, while it is the eigenstate only there. One may think that an appropriate change of the variable which brings $x = +\infty$ to some finite coordinate makes the wave function rapidly oscillate near the boundary of the region. To remedy this, we factorize the oscillating part of the wave function.

Before performing the factorization, let us remove the effect of CP violation in the broken phase by a unitary transformation of the two-spinor. Introducing a unitary matrix

$$U = \frac{1}{\sqrt{2}} \begin{pmatrix} i & -i \\ \mathrm{e}^{i\theta_0} & \mathrm{e}^{i\theta_0} \end{pmatrix}, \tag{2.13}$$

and transforming the spinor as

$$\begin{pmatrix} \tilde{\psi}_1(x) \\ \tilde{\psi}_3(x) \end{pmatrix} = U^{-1} \begin{pmatrix} \psi_1(x) \\ \psi_3(x) \end{pmatrix}, \qquad \begin{pmatrix} \tilde{\psi}_4(x) \\ \tilde{\psi}_2(x) \end{pmatrix} = U^{*-1} \begin{pmatrix} \psi_4(x) \\ \psi_2(x) \end{pmatrix}, \tag{2.14}$$

the Dirac equation is reduced to

$$\partial_x \begin{pmatrix} \tilde{\psi}_1(x) \\ \tilde{\psi}_3(x) \end{pmatrix} = \begin{pmatrix} \xi f(x) & -i[\sigma\epsilon + \xi g(x)] \\ -i[\sigma\epsilon - \xi g(x)] & -\xi f(x) \end{pmatrix} \begin{pmatrix} \tilde{\psi}_1(x) \\ \tilde{\psi}_3(x) \end{pmatrix}, \tag{2.15}$$

$$\partial_x \begin{pmatrix} \tilde{\psi}_4(x) \\ \tilde{\psi}_2(x) \end{pmatrix} = \begin{pmatrix} -\xi f(x) & -i[\sigma\epsilon + \xi g(x)] \\ -i[\sigma\epsilon - \xi g(x)] & \xi f(x) \end{pmatrix} \begin{pmatrix} \tilde{\psi}_4(x) \\ \tilde{\psi}_2(x) \end{pmatrix}, \tag{2.16}$$

where

$$\xi f(x) \equiv \xi(x)\cos(\theta(x) - \theta_0), \qquad \xi g(x) \equiv \xi(x)\sin(\theta(x) - \theta_0). \tag{2.17}$$

These satisfy the boundary conditions

$$\begin{aligned} f(x) &\to 1, \quad g(x) \to 0, \qquad \text{as } x \to +\infty \\ f(x) &\to 0, \quad g(x) \to 0, \qquad \text{as } x \to -\infty. \end{aligned}$$

In the following, we consider only the positive frequency wave ($\sigma = +$) for definiteness. For the boundary condition we concern, the wave functions behave as, at $x \sim +\infty$,

$$\tilde{\psi}_a(x) \sim C_a \mathrm{e}^{\alpha x}. \tag{2.18}$$

The asymptotic form of (2.15) yields

$$(\xi - \alpha)C_1\mathrm{e}^{\alpha x} = i\epsilon C_3 \mathrm{e}^{\alpha x}, \qquad (\xi + \alpha)C_3\mathrm{e}^{\alpha x} = -i\epsilon C_1\mathrm{e}^{\alpha x},$$

which gives

$$C_3 = \frac{\xi - \alpha}{i\epsilon} C_1. \tag{2.19}$$

Similarly we have

$$C_4 = \frac{\xi - \alpha}{i\epsilon} C_2. \tag{2.20}$$

Now we factorize the wave function as

$$\begin{aligned} \tilde{\psi}_1(x) &= C_1\mathrm{e}^{\alpha x}\chi_1(x), \\ \tilde{\psi}_2(x) &= C_2\mathrm{e}^{\alpha x}\chi_2(x), \\ \tilde{\psi}_3(x) &= \frac{\xi - \alpha}{i\epsilon} C_1\mathrm{e}^{\alpha x}\chi_3(x), \\ \tilde{\psi}_4(x) &= \frac{\xi - \alpha}{i\epsilon} C_2\mathrm{e}^{\alpha x}\chi_4(x). \end{aligned} \tag{2.21}$$

The boundary condition is now

$$\chi_a(x = +\infty) = 1. \tag{2.22}$$

In terms of χ_a, the Dirac equation (2.15) and (2.16) is expressed as

$$\begin{aligned} \chi_1'(x) &= (\xi - \alpha)(\chi_1(x) - \chi_3(x)) + \xi(f(x) - 1)\chi_1(x) - \frac{\xi(\xi - \alpha)}{\epsilon} g(x)\chi_3(x), \\ \chi_3'(x) &= (\xi + \alpha)(\chi_1(x) - \chi_3(x)) - \xi(f(x) - 1)\chi_3(x) - \frac{\xi(\xi + \alpha)}{\epsilon} g(x)\chi_1(x), \end{aligned} \tag{2.23}$$

$$\begin{aligned} \chi_2'(x) &= (\xi - \alpha)(\chi_2(x) - \chi_4(x)) + \xi(f(x) - 1)\chi_2(x) + \frac{\xi(\xi - \alpha)}{\epsilon} g(x)\chi_4(x), \\ \chi_4'(x) &= (\xi + \alpha)(\chi_2(x) - \chi_4(x)) - \xi(f(x) - 1)\chi_4(x) + \frac{\xi(\xi + \alpha)}{\epsilon} g(x)\chi_2(x). \end{aligned} \tag{2.24}$$

Note that the right-hand sides of the above equations vanish at $x = +\infty$.

2.3 Reflection and transmission coefficients

To determine the transmission and reflection coefficients, we need their asymptotic forms. Suppose that the wave function behaves as, at $x \sim -\infty$,

$$\psi_a(x) \sim A_a \mathrm{e}^{\beta x} + B_a \mathrm{e}^{-\beta x}, \tag{2.25}$$

where $\beta = i\epsilon$. Then the incident and reflection currents are given by

$$\begin{array}{ll} \left(j_L^3\right)^{\rm inc} = |A_4|^2 - |A_3|^2, & \left(j_R^3\right)^{\rm inc} = |A_1|^2 - |A_2|^2, \\ \left(j_L^3\right)^{\rm refl} = |B_4|^2 - |B_3|^2, & \left(j_R^3\right)^{\rm refl} = |B_1|^2 - |B_2|^2. \end{array} \tag{2.26}$$

In the asymptotic region ($x \sim -\infty$), the coefficients A_a and B_a are given by

$$\begin{aligned} A_a &= \frac{\mathrm{e}^{-\beta x}}{2}\left(\psi_a(x) + \frac{1}{\beta}\psi_a'(x)\right), \\ B_a &= \frac{\mathrm{e}^{\beta x}}{2}\left(\psi_a(x) - \frac{1}{\beta}\psi_a'(x)\right). \end{aligned}$$

Strictly speaking, these are not independent of x at any finite x. However, we shall use these expressions to calculate the transmission and reflection coefficients for so large x that they stay almost constant.

Because of (2.14),

$$\begin{aligned} \begin{pmatrix} \psi_1 \\ \psi_3 \end{pmatrix} &= U \begin{pmatrix} \tilde\psi_1 \\ \tilde\psi_3 \end{pmatrix} = \begin{pmatrix} \frac{i}{\sqrt{2}}(\tilde\psi_1 - \tilde\psi_3) \\ \frac{\mathrm{e}^{i\theta_0}}{\sqrt{2}}(\tilde\psi_1 + \tilde\psi_3) \end{pmatrix}, \\ \begin{pmatrix} \psi_4 \\ \psi_2 \end{pmatrix} &= U^* \begin{pmatrix} \tilde\psi_4 \\ \tilde\psi_2 \end{pmatrix} = \begin{pmatrix} \frac{i}{\sqrt{2}}(\tilde\psi_2 - \tilde\psi_4) \\ \frac{\mathrm{e}^{-i\theta_0}}{\sqrt{2}}(\tilde\psi_2 + \tilde\psi_4) \end{pmatrix}. \end{aligned}$$

In terms of $\chi_a(x)$, the "constants" are expressed as

$$\begin{aligned} |A_1|^2 &= \frac{|C_1|^2}{8}\left|(1+\frac{\alpha}{\beta})\chi_1(x) + \frac{1}{\beta}\chi_1'(x) - \frac{\xi-\alpha}{\beta}\left[(1+\frac{\alpha}{\beta})\chi_3(x) + \frac{1}{\beta}\chi_3'(x)\right]\right|^2, \\ |A_3|^2 &= \frac{|C_1|^2}{8}\left|(1+\frac{\alpha}{\beta})\chi_1(x) + \frac{1}{\beta}\chi_1'(x) + \frac{\xi-\alpha}{\beta}\left[(1+\frac{\alpha}{\beta})\chi_3(x) + \frac{1}{\beta}\chi_3'(x)\right]\right|^2, \\ |A_2|^2 &= \frac{|C_2|^2}{8}\left|(1+\frac{\alpha}{\beta})\chi_2(x) + \frac{1}{\beta}\chi_2'(x) + \frac{\xi-\alpha}{\beta}\left[(1+\frac{\alpha}{\beta})\chi_4(x) + \frac{1}{\beta}\chi_4'(x)\right]\right|^2, \\ |A_4|^2 &= \frac{|C_2|^2}{8}\left|(1+\frac{\alpha}{\beta})\chi_2(x) + \frac{1}{\beta}\chi_2'(x) - \frac{\xi-\alpha}{\beta}\left[(1+\frac{\alpha}{\beta})\chi_4(x) + \frac{1}{\beta}\chi_4'(x)\right]\right|^2, \end{aligned} \tag{2.27}$$

and

$$
\begin{aligned}
|B_1|^2 &= \frac{|C_1|^2}{8}\left|(1-\frac{\alpha}{\beta})\chi_1(x) - \frac{1}{\beta}\chi_1'(x) - \frac{\xi-\alpha}{\beta}\left[(1-\frac{\alpha}{\beta})\chi_3(x) - \frac{1}{\beta}\chi_3'(x)\right]\right|^2, \\
|B_3|^2 &= \frac{|C_1|^2}{8}\left|(1-\frac{\alpha}{\beta})\chi_1(x) - \frac{1}{\beta}\chi_1'(x) + \frac{\xi-\alpha}{\beta}\left[(1-\frac{\alpha}{\beta})\chi_3(x) - \frac{1}{\beta}\chi_3'(x)\right]\right|^2, \\
|B_2|^2 &= \frac{|C_2|^2}{8}\left|(1-\frac{\alpha}{\beta})\chi_2(x) - \frac{1}{\beta}\chi_2'(x) + \frac{\xi-\alpha}{\beta}\left[(1-\frac{\alpha}{\beta})\chi_4(x) - \frac{1}{\beta}\chi_4'(x)\right]\right|^2, \\
|B_4|^2 &= \frac{|C_2|^2}{8}\left|(1-\frac{\alpha}{\beta})\chi_2(x) - \frac{1}{\beta}\chi_2'(x) - \frac{\xi-\alpha}{\beta}\left[(1-\frac{\alpha}{\beta})\chi_4(x) - \frac{1}{\beta}\chi_4'(x)\right]\right|^2,
\end{aligned}
\tag{2.28}
$$

where $'$ denotes the derivative with respect to x. On the other hand, the transmitted currents are

$$
\begin{aligned}
\left(j_L^3\right)^{\rm trans} &= \frac{1}{2}|C_2|^2\left|1-\frac{\xi-\alpha}{\beta}\right|^2 - \frac{1}{2}|C_1|^2\left|1+\frac{\xi-\alpha}{\beta}\right|^2, \\
\left(j_R^3\right)^{\rm trans} &= \frac{1}{2}|C_1|^2\left|1-\frac{\xi-\alpha}{\beta}\right|^2 - \frac{1}{2}|C_2|^2\left|1+\frac{\xi-\alpha}{\beta}\right|^2.
\end{aligned}
\tag{2.29}
$$

Equipped with these coefficients, we are ready to evaluate the transmission and reflection coefficients.

The transmission and reflection coefficients of the chiral fermions are defined by

$$
T_{L\to L(R)} = \left.\frac{\left(j_{L(R)}^3\right)^{\rm trans}}{\left(j_L^3\right)^{\rm inc}}\right|_{\left(j_R^3\right)^{\rm inc}=0}, \tag{2.30}
$$

$$
T_{R\to L(R)} = \left.\frac{\left(j_{L(R)}^3\right)^{\rm trans}}{\left(j_R^3\right)^{\rm inc}}\right|_{\left(j_L^3\right)^{\rm inc}=0}, \tag{2.31}
$$

$$
R_{R(L)\to L(R)} = -\left.\frac{\left(j_{L(R)}^3\right)^{\rm refl}}{\left(j_{R(L)}^3\right)^{\rm inc}}\right|_{\left(j_{L(R)}^3\right)^{\rm inc}=0}. \tag{2.32}
$$

The condition $\left(j_{L(R)}^3\right)^{\rm inc} = 0$ is realized by appropriately choosing the ratio of C_1 and C_2. For example, to realize $\left(j_R^3\right)^{\rm inc} = 0$, we take

$$
\begin{aligned}
|C_1|^2 &= \left|(1+\frac{\alpha}{\beta})\chi_2(x) + \frac{1}{\beta}\chi_2'(x) + \frac{\xi-\alpha}{\beta}\left[(1+\frac{\alpha}{\beta})\chi_4(x) + \frac{1}{\beta}\chi_4'(x)\right]\right|^2, \\
|C_2|^2 &= \left|(1+\frac{\alpha}{\beta})\chi_1(x) + \frac{1}{\beta}\chi_1'(x) - \frac{\xi-\alpha}{\beta}\left[(1+\frac{\alpha}{\beta})\chi_3(x) + \frac{1}{\beta}\chi_3'(x)\right]\right|^2,
\end{aligned}
\tag{2.33}
$$

so that $\left(j_R^3\right)^{\rm inc} = |A_1|^2 - |A_2|^2 = 0$. Given these $|C_i|^2$, (2.30)$\sim$(2.32) yield the chiral transmission and reflection coefficients by use of (2.26) and (2.29).

3 Numerical Analysis

To realize the boundary condition (2.22) at $x = \infty$ on a computer, we change the variable of infinite range to another of half-infinite range. For definiteness, we take the following new variable

$$y = \mathrm{e}^{-az} = \mathrm{e}^{-x} \in (0, \infty). \tag{3.1}$$

This transforms $\frac{d}{dx} \mapsto -y\frac{d}{dy}$ so that it brings the singularity at $y = 0$ into the Dirac equation. As we show below, the right-hand sides of (2.23) and (2.24) well behave to cancel such singularity.

The bubble wall connecting the broken and the symmetric phase is expected to behave as

$$\begin{array}{ll} \rho(z) \sim 1 + \mathrm{e}^{-bz}, & \text{as } z \to +\infty \\ \rho(z) \sim \mathrm{e}^{b'z}, & \text{as } z \to -\infty \end{array} \tag{3.2}$$

where $b(> 0)$ and $b'(> 0)$ will be order of the Higgs masses. Hence if we choose a to be smaller than the Higgs mass ($a < b$), the potentials in the Dirac equation behave as, at $y \sim 0$ ($x \sim +\infty$),

$$f(y) \sim 1 + y^\mu, \qquad g(y) \sim y^\nu,$$

with $\mu, \nu > 1$. Now put

$$f(y) = 1 + y^\mu \sum_{n=0}^{\infty} f_n y^n, \qquad g(y) = y^\nu \sum_{n=0}^{\infty} g_n y^n. \qquad (f_0 \neq 0, g_0 \neq 0)$$

To find the asymptotic behaviors of $\chi_1(y)$ and $\chi_3(y)$, expand them as

$$\begin{array}{ll} \chi_1(y) = 1 + y^\rho \sum_{n=0}^{\infty} a_n y^n, & (\mathbf{R} \ni \rho > 0, a_0 \neq 0) \\ \chi_3(y) = 1 + y^\sigma \sum_{n=0}^{\infty} b_n y^n. & (\mathbf{R} \ni \sigma > 0, b_0 \neq 0) \end{array} \tag{3.3}$$

Then (2.23) in terms of y yield

$$\begin{aligned} -\sum_{n=0}^{\infty}(\rho+n)a_n y^n &= (\xi-\alpha)\left(\sum_{n=0}^{\infty} a_n y^n - y^{\sigma-\rho}\sum_{n=0}^{\infty} b_n y^n\right) + \xi\, y^{\mu-\rho}\sum_{n=0}^{\infty} f_n y^n (1 + y^\rho \sum_{n=0}^{\infty} a_n y^n) \\ &\quad -\frac{\xi(\xi-\alpha)}{\epsilon} y^{\nu-\rho}\sum_{n=0}^{\infty} g_n y^n (1 + y^\sigma \sum_{n=0}^{\infty} b_n y^n), \end{aligned} \tag{3.4}$$

$$\begin{aligned} -\sum_{n=0}^{\infty}(\sigma+n)b_n y^n &= (\xi+\alpha)\left(y^{\rho-\sigma}\sum_{n=0}^{\infty} a_n y^n - \sum_{n=0}^{\infty} b_n y^n\right) - \xi\, y^{\mu-\sigma}\sum_{n=0}^{\infty} f_n y^n (1 + y^\sigma \sum_{n=0}^{\infty} b_n y^n) \\ &\quad -\frac{\xi(\xi+\alpha)}{\epsilon} y^{\nu-\sigma}\sum_{n=0}^{\infty} g_n y^n (1 + y^\rho \sum_{n=0}^{\infty} a_n y^n). \end{aligned} \tag{3.5}$$

When $\mu < \rho, \sigma$ or $\nu < \rho, \sigma$, the right-hand sides of the both equations have singularities.[1] When $\mu > \rho, \sigma$ and $\nu > \rho, \sigma$, we must have $\rho = \sigma$. This is because, otherwise, the right-hand side of either (3.4) or (3.5) has a singularity, $b_0 y^{\sigma-\rho}$ or $a_0 y^{\rho-\sigma}$, which cannot vanish because of $a_0 \neq 0$ and $b_0 \neq 0$. Then $O(y^0)$ terms give

$$\begin{aligned}(\xi - \alpha + \rho)a_0 - (\xi - \alpha)b_0 &= 0, \\ (\xi + \alpha)a_0 - (\xi + \alpha - \rho)b_0 &= 0.\end{aligned}$$

To have nontrivial a_0 and b_0,

$$(\xi - \alpha + \rho)(\xi + \alpha - \rho) - (\xi - \alpha)(\xi + \alpha) = \rho(2\alpha - \rho) = 0,$$

which has no real solution $\rho > 0$. Therefore to avoid any singularity in the right-hand sides, we are left with two possibilities:

$$\rho = \sigma = \mu \leq \nu, \qquad \text{or} \qquad \rho = \sigma = \nu \leq \mu. \tag{3.6}$$

In these cases, the lowest order equations determine a_0 and b_0 in terms of f_0 and/or g_0. Needless to say, the same argument also applies to the remaining components of the Dirac equation.

Thus the Dirac equations in terms of y are free from any singularity, so that they can be numerically integrated by use of a standard algorithm such as the Runge-Kutta method. Now we summarize our procedure to calculate the chiral reflection coefficients:

1. Prepare the potential $f(y)$ and $g(y)$. These would be determined by the model we choose through the equations of motion.

2. Integrate the Dirac equation

$$\begin{aligned}-y\frac{d\chi_1(y)}{dy} &= (\xi - \alpha)(\chi_1(y) - \chi_3(y)) + \xi(f(y) - 1)\chi_1(y) - \frac{\xi(\xi - \alpha)}{\epsilon}g(y)\chi_3(y), \\ -y\frac{d\chi_3(y)}{dy} &= (\xi + \alpha)(\chi_1(y) - \chi_3(y)) - \xi(f(y) - 1)\chi_3(y) - \frac{\xi(\xi + \alpha)}{\epsilon}g(y)\chi_1(y),\end{aligned} \tag{3.7}$$

$$\begin{aligned}-y\frac{d\chi_2(y)}{dy} &= (\xi - \alpha)(\chi_2(y) - \chi_4(y)) + \xi(f(y) - 1)\chi_2(y) + \frac{\xi(\xi - \alpha)}{\epsilon}g(y)\chi_4(y), \\ -y\frac{d\chi_4(y)}{dy} &= (\xi + \alpha)(\chi_2(y) - \chi_4(y)) - \xi(f(y) - 1)\chi_4(y) + \frac{\xi(\xi + \alpha)}{\epsilon}g(y)\chi_2(y),\end{aligned} \tag{3.8}$$

starting from the boundary condition $\chi_a(y = 0) = 1$ to large y with a step Δy. Within each step, one can control the precision by choosing sufficiently small meshes or using quality control algorithm which automatically divides the mesh until the desired precision is reached.

[1] One may think that in (3.4) when $\mu = \nu < \rho$, they cancel with each other if $\epsilon f_0 = (\xi - \alpha)g_0$. But this is impossible for real f_0 and g_0.

3. At the end of each step, evaluate the reflection and transmission coefficients.

4. Proceed to larger y, until the relative error in the coefficients comes to be smaller than the prescribed precision.

We shall see how this program works in the next section.

4 Examples

Here we take the following potentials to illustrate the calculation of the chiral reflection coefficients. The chiral charge flux can be obtained by the procedure outlined in [4] integrating the reflection coefficients multiplied by the statistical distribution functions of the fermions.

(i) $\xi(x)\mathrm{e}^{i\theta(x)} = \xi\dfrac{1+\tanh x}{2}\exp\left[i\Delta\theta\dfrac{1-\tanh x}{2}\right]$.
This with $\Delta\theta = -\pi$ was taken in [2].

(ii) $\xi(x)\mathrm{e}^{i\theta(x)} = \xi\dfrac{1+\tanh x}{2}\mathrm{e}^{i\theta(x)}$,
with $\theta(x)$ being the solution to the equations of motion of the gauge-Higgs system, depicted in Fig. 2 of [5], satisfying $\theta_0 = \theta(y=0) = 1$ and $\theta(y=\infty) = 0$.

(iii) $\xi(x)\mathrm{e}^{i\theta(x)} = \xi\dfrac{1+\tanh x}{2}\mathrm{e}^{i\theta(x)}$,
with $\theta(x)$ being the solution to the equations of motion of the gauge-Higgs system, depicted in Fig. 3 of [5], satisfying $\theta(y=0) = \theta(y=\infty) = 0$.

In the charge transport scenario, the generated baryon number density is given by [2]

$$\frac{n_B}{s} \simeq \mathcal{N}\frac{100}{\pi^2 g_*}\,\kappa\alpha_W^4\,\frac{F_Y\tau}{uT^2}, \tag{4.1}$$

where $\mathcal{N}$ is the model-dependent factor of $O(1)$, g_* is the radiation degrees of freedom at T_C and is of $O(100)$, $\kappa\alpha_W^4$ is the sphaleron transition rate in the symmetric phase and is of $O(10^{-6})$ and u is the wall velocity. τ stands for the transport time, which is given by the average time the reflected fermion spends in the plasma before caught up with the bubble wall. It is expected to be of $O(10) \sim O(1000)$ times the thermal correlation lengths, depending on the wall velocity, if the forward scattering is enhanced. In the original scenario, the weak hypercharge was taken as the chiral charge injected into the symmetric phase. In the following, we mean by the chiral charge flux the dimensionless quantity normalized as

$$\frac{F_Q}{uT^3(Q_L - Q_R)}. \tag{4.2}$$

case (i)

In terms of the variable y, the potentials are written as

$$f(y) = \frac{1}{1+y^2}\cos\left(\frac{\Delta\theta\, y^2}{1+y^2}\right), \qquad g(y) = \frac{1}{1+y^2}\sin\left(\frac{\Delta\theta\, y^2}{1+y^2}\right). \tag{4.3}$$

Now we take $\Delta\theta = -\pi$. To show how the program in the previous section works, we calculated the reflection and transmission coefficients of the left-handed fermion for $\xi = 1$ and $\epsilon = 1.2$. The result is listed in Table 1 for first several y. The column 'unitarity'

y	$R_{L\to R}$	$T_{L\to L} + T_{L\to R}$	unitarity
20	$5.42508153 \times 10^{-1}$	$4.57493406 \times 10^{-1}$	1.00000156
40	$5.42731549 \times 10^{-1}$	$4.57268549 \times 10^{-1}$	1.00000010
60	$5.42819216 \times 10^{-1}$	$4.57180804 \times 10^{-1}$	1.00000002
80	$5.42830565 \times 10^{-1}$	$4.57169442 \times 10^{-1}$	1.00000001
100	$5.42826265 \times 10^{-1}$	$4.57173738 \times 10^{-1}$	1.00000000
120	$5.42820329 \times 10^{-1}$	$4.57179672 \times 10^{-1}$	1.00000000
140	$5.42815576 \times 10^{-1}$	$4.57184425 \times 10^{-1}$	1.00000000
160	$5.42812238 \times 10^{-1}$	$4.57187764 \times 10^{-1}$	1.00000000
180	$5.42810021 \times 10^{-1}$	$4.57189980 \times 10^{-1}$	1.00000000
200	$5.42808603 \times 10^{-1}$	$4.57191398 \times 10^{-1}$	1.00000000
220	$5.42807730 \times 10^{-1}$	$4.57192270 \times 10^{-1}$	1.00000000
240	$5.42807222 \times 10^{-1}$	$4.57192778 \times 10^{-1}$	1.00000000
260	$5.42806955 \times 10^{-1}$	$4.57193046 \times 10^{-1}$	1.00000000
280	$5.42806844 \times 10^{-1}$	$4.57193157 \times 10^{-1}$	1.00000000
300	$5.42806833 \times 10^{-1}$	$4.57193167 \times 10^{-1}$	1.00000000

Table 1: The reflection and transmission coefficients of the left-handed fermion. These should become constants for $y \sim \infty$.

means the sum of the two columns left to it. This shows that to get the precision of four digits, it is sufficient to integrate the equations up to $y = 100$, which is amount to $x = -\ln 100 \simeq -4.6052$ and is regarded far from the bubble wall. In this case, one can obtain the same data of $\Delta R = R_{R\to L} - R_{L\to R}$ as a function of (ϵ, ξ) as shown in Fig. 2 of [2].

For $\Delta\theta = 0.001$, we confirmed that our numerical method yields the same ΔR as that obtained by the perturbative method in [4]. For $\Delta\theta = -1$, which is equivalent to the profile

$$\xi(x)\mathrm{e}^{i\theta(x)} = \xi\frac{1+\tanh x}{2}\exp\left[i\frac{1+\tanh x}{2}\right], \tag{4.4}$$

up to the unitary transformation (2.14), we calculated ΔR by the numerical method developed here. The chiral charge fluxes for various mass and wall width are depicted in

Fig. 1.

case (ii)

In this case, $\theta_0 = 1$ and the maximum of $g(x)$ is about 0.4, which is comparable with $f(x)$ at the same x. So we did not evaluated the chiral charge flux in [5], using our perturbative method[4]. This profile, which is a solution to the equations of motion to the gauge-Higgs system with the kink-type $\rho(x)$, indicates that $\theta(x)$ is no longer proportional to the kink when θ_0 is $O(1)$. This should be compared with the profile (4.4), which satisfies the same boundary conditions. We performed the numerical calculation of the chiral charge flux, which is given in Fig. 2. This shows that this profile slightly enhances the flux over the profile employed in [2] by about a factor of 2. The former is about 80% larger near the peak, and decreases more slowly for large mass or thick wall than the latter.

case (iii)

Although the maximum of $\theta(x)$ reaches 0.37, the potential $f(x)$ has a kink-like shape and $g(x)$ is sufficiently small as shown in Fig. 4 of [5]. We expected that the perturbative method is applicable to this case and evaluated the chiral charge flux, depicted in Fig. 5 of [5]. To confirm this, we calculated ΔR for several (ϵ, ξ). One of the results is given in Fig. 3 for $\xi = 0.4$ and $m_0 = 1$. This shows that the perturbative method was a good approximation in this case.

5 Discussions

We proposed a numerical method to solve the scattering problem of the Dirac equation in the background of any CP-violating bubble wall. By use of it, one can evaluate the reflection coefficients of chiral fermions to any precision. This will be a powerful tool to analyze electroweak baryogenesis based on the charge transport scenario.

Whether the charge transport or the spontaneous mechanism is effective will be determined by the dynamics of the EWPT. Recent study of the standard model at finite temperature[6] suggests that the first order nature of the EWPT is stronger than that expected from the one-loop calculation of the effective potential. Even though efficient electroweak baryogenesis requires some extension of the Higgs sector to incorporate spatially varying CP phase, this fact would mean that the bubble wall would be thinner than naively expected from the lowest order effective potential, so that the charge transport scenario would play a crucial role in baryogenesis.

The profiles of the bubble wall which we took in this paper have the kink-type $\rho(x)$. In fact, they should be determined by the dynamics, and we have shown that the modulus of the Higgs could be distorted from the kink, when $\theta(x)$ is not small for the choice of

the effective potential which has a kink-type $\rho(x)$ for $\theta = 0$[7]. For such a profile, we can evaluate the flux precisely, by taking sufficiently small a.

References

[1] For a review see, A. Cohen, D. Kaplan and A. Nelson, Ann. Rev. Nucl. Part. Sci. **43** (1993) 27.

[2] A. Nelson, D. Kaplan and A. Cohen, Nucl. Phys. **B373** (1992) 453.

[3] K. Funakubo, A. Kakuto, S. Otsuki, K. Takenaga and F. Toyoda, Phys. Rev. **D50** (1994) 1105.

[4] K. Funakubo, A. Kakuto, S. Otsuki, K. Takenaga and F. Toyoda, Prog. Theor. Phys. **93** (1995) 1067.

[5] K. Funakubo, A. Kakuto, S. Otsuki, K. Takenaga and F. Toyoda, Prog. Theor. Phys. **94** (1995) 845.

[6] K. Jansen, hep-lat/9509018 and references therein.

[7] K. Funakubo, A. Kakuto, S. Otsuki and F. Toyoda, in preparation.

Figure Captions

Fig.1: Contour plot of the chiral charge flux, $\log_{10}[-F_Q/(uT^3(Q_L - Q_R))]$ for the example (i) with $\theta_0 = -1$. Here we take $u = 0.1$ and $T = 100$GeV.

Fig.2: Contour plot of the chiral charge flux, normalized as $\log_{10}[-F_Q/(uT^3(Q_L - Q_R))]$ for the example (ii), given in Fig. 2 of [5]. Here we take the same u and T as Fig. 1.

Fig.3: ΔR for the profile given in Fig. 3 of [5]. Here we take $\xi = 0.4$ and $m_0 = 1$. The solid line represents the numerical result obtained here. The dashed line stands for the previous result based on the perturbative method.

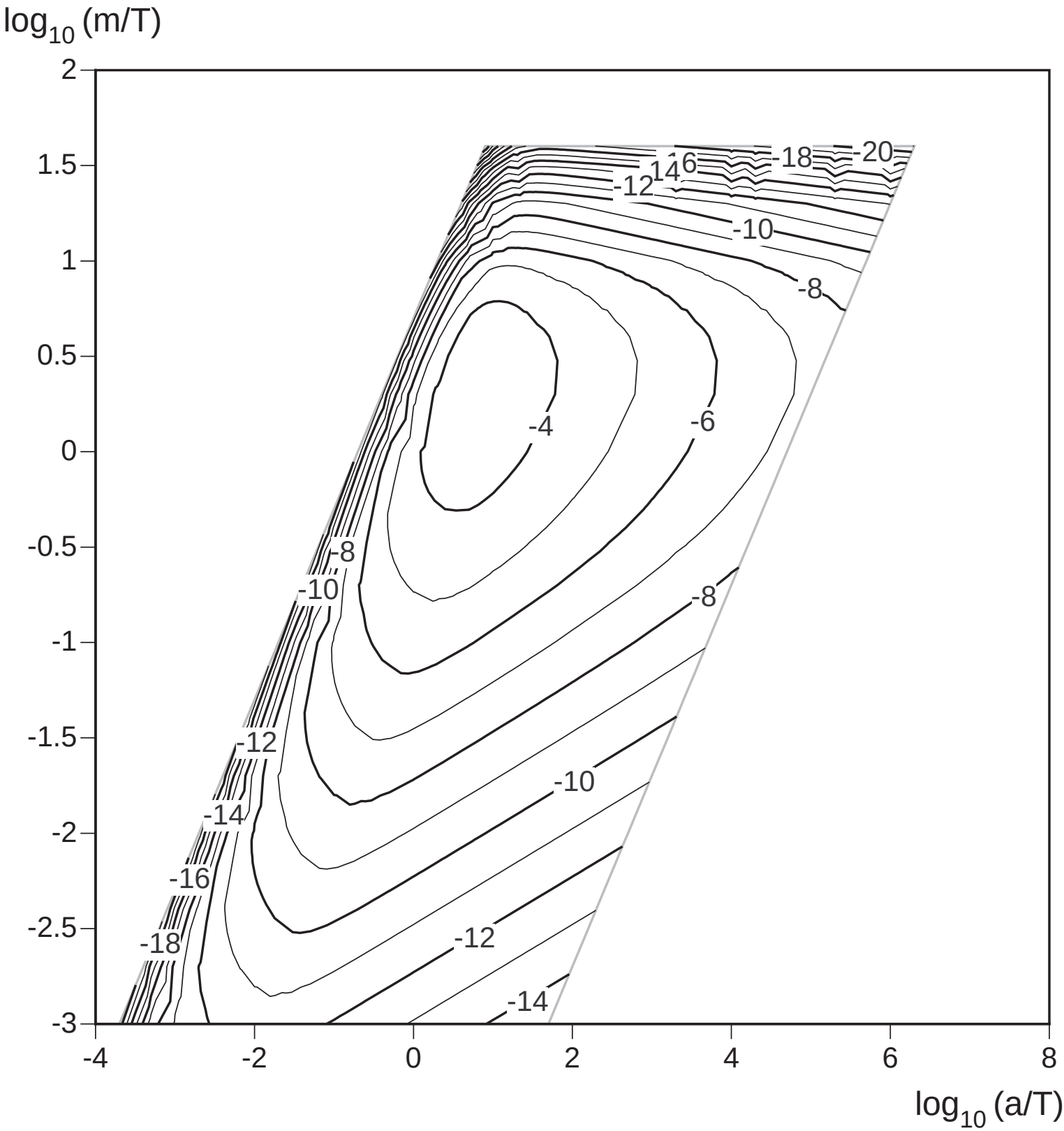
log10 (m/T)
2
1.5
1
0.5
0
-0.5
-1
-1.5
-2
-2.5
-3
-4
-2
0
2
4
6
8
log10 (a/T)
-4
-6
-8
-10
-12
-14
-16
-18
-20

Fig.1

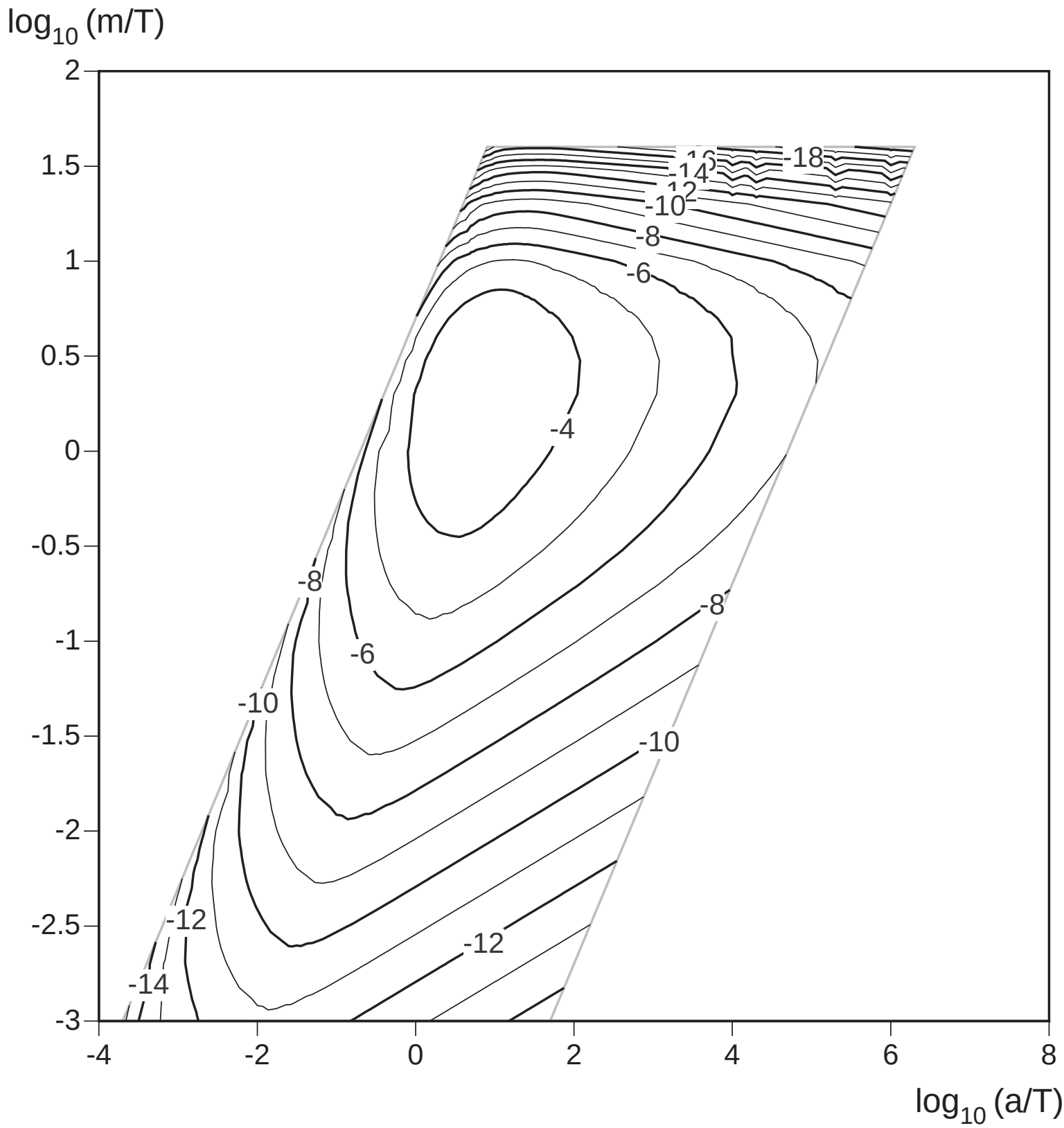
log10 (m/T)
2
1.5
1
0.5
0
-0.5
-1
-1.5
-2
-2.5
-3
-4
-2
0
2
4
6
8
log10 (a/T)
-18
-14
-12
-10
-8
-6
-4
-8
-6
-10
-8
-10
-12
-12
-14

Fig.2

Fig.3